2D Materials

OPEN ACCESS

RECEIVED
7 November 2019

REVISED
24 January 2020

ACCEPTED FOR PUBLICATION
4 February 2020

PUBLISHED
28 February 2020

PAPER

A system for the deterministic transfer of 2D materials under inert environmental conditions

Patricia Gant[1,5], Felix Carrascoso[1,5], Qinghua Zhao[1,2,3], Yu Kyoung Ryu[1], Michael Seitz[4], Ferry Prins[4], Riccardo Frisenda[1] and Andres Castellanos-Gomez[1]

[1] Materials Science Factory, Instituto de Ciencia de Materiales de Madrid, Consejo Superior de Investigaciones Científicas, 28049 Madrid, Spain
[2] State Key Laboratory of Solidification Processing, Northwestern Polytechnical University, Xi'an 710072, People's Republic of China
[3] Key Laboratory of Radiation Detection Materials and Devices, Ministry of Industry and Information Technology, Xi'an 710072, People's Republic of China
[4] Condensed Matter Physics Center (IFIMAC), Autonomous University of Madrid, 28049 Madrid, Spain
[5] These authors contributed equally to this work

E-mail: riccardo.frisenda@csic.es **and** andres.castellanos@csic.es

Keywords: deterministic transfer, inert atmosphere, experimental setup, gloveless anaerobic chamber, heterostructure assembly

Supplementary material for this article is available online

Abstract

The isolation of air-sensitive two-dimensional (2D) materials and the race to achieve a better control of the interfaces in van der Waals heterostructures has pushed the scientific community towards the development of experimental setups that allow to exfoliate and transfer 2D materials under inert atmospheric conditions. These systems are typically based on over pressurized N_2 of Ar gloveboxes that require the use of very thick gloves to operate within the chamber or the implementation of several motorized micro-manipulators. Here, we set up a deterministic transfer system for 2D materials within a gloveless anaerobic chamber. Unlike other setups based on over-pressurized gloveboxes, in our system the operator can manipulate the 2D materials within the chamber with bare hands. This experimental setup allows us to exfoliate 2D materials and to deterministically place them at a desired location with accuracy in a controlled O_2-free and very low humidity (<2% RH) atmosphere. We illustrate the potential of this system to work with air-sensitive 2D materials by comparing the stability of black phosphorus and perovskite flakes inside and outside the anaerobic chamber.

The deterministic transfer methods, that allow for the placement of 2D materials onto a user defined specific location with an unprecedented degree of accuracy and reliability, are at the origin of the large success of two-dimensional (2D) materials research [1–6]. This control over the position of the transferred flakes has been exploited to fabricate devices with rather complex architectures as well as to assemble artificial stacks of dissimilar 2D materials to build-up the so-called van der Waals heterostructures [7–10]. In particular, deterministic placement methods have enabled the fabrication of 2D-based samples fully-encapsulated between insulating layers of hexagonal boron nitride (hBN), exhibiting record-high electronic performance that allowed for the observation of intriguing physical phenomena [4, 6]. Nonetheless, there are two main challenges of this line of research: (1) how to achieve a better control of the interfaces [11–13], (2) how to handle air-sensitive 2D materials [14, 15]. Indeed, the continuous race to increase the performances of 2D devices and the isolation of novel unstable 2D materials under atmospheric exposure, have pushed towards the development of experimental setups where the transfer process can be carried out under controlled environmental conditions [14, 16, 17]. Although several research groups have implemented their own systems based on N^2 or Ar glove-boxes, the literature is lacking of comprehensive technical articles providing enough details for reproducing such systems by other groups. Moreover, these glove-box-based systems can be difficult to operate as delicate manual operation (e.g. mechanical exfoliation, handling small substrates with tweezers, …) have to be carried out while wearing thick gloves. In order to overcome this handicap, some systems are fully motorized and thus do not require any manual operation within the glovebox,

Table 1. List of all the setup components, which includes the part numbers and the prices.

Component	Description	Part number	Distributor	Price
Chamber[a]	Bactronez 12.5 CU.FT.I 354 L, anaerobic chamber, 300 plate capacity	BAAEZ22	Bactron-Sheldon manufacturing	14 700.00 €
Optomechanical component	Breadboard, ferromagnetic steel	1BS-2040-015	Standa	130.00 €
	Post ¾″ dia stainless posts, vertical post 18″	39-353	Edmund optics	57.00 €
	Mounting Post Base, Ø2.48″ × 0.40″ thick	PB1	Thorlabs	22.44 €
Zoom lens	Focusing, coarse/fine movement, 50 mm diameter thru hole, rack and pinion	54-792	Edmund optics	355.00 €
	EOS camera adapter	89-862	Edmund optics	75.00 €
	3.0× mini-camera tube	89-877	Edmund optics	725.00 €
	7× zoom module, manual	89-878	Edmund optics	750.00 €
	Lower module w/in-line illumination	89-888	Edmund optics	275.00 €
	4.0× lower lens	89-903	Edmund optics	275.00 €
	Fiber optic light guide adapter	89-919	Edmund optics	125.00 €
	Fiber optic light guide adapter to 10 mm	89-920	Edmund optics	55.00 €
Illumination	Bench power supply, linear, adjustable, 1 output, 0 V, 30 V, 0 A, 5 A	72-2690	Farnell	71.34 €
	LED, white, through hole, T-3 (10 mm), 20 mA, 3.5 V, 8 cd	VAOL-10GWY4	Farnell	0.47 €
	Quartz Tungsten-Halogen Lamp	QTH10	Thorlabs	157.58 €
Oxygen meter	Oxygen detector	AR8100	Smart sensor	81.10 €
Stages	Manual *XY* linear stage	MAXY-B60L-13	Optics focus solutions	72.10 €
	Manual *XYZ* stage	MAXYZ-60L	Optics focus solutions	164.00 €
	Square neodymiun magnets N52 10 × 10 × 4 mm	Amazon shop	Magnetastico	18.99 €
	Ø1.40″ manual mini-series rotation stage, metric	MSRP01/M	Thorlabs	66.53 €
Camera	Canon EOS 1300D—18 Mp (3″ screen, Full HD, NFC, WiFi)		Canon	324.00 €
	Power supply for Canon EOS 1300D-ca. 3 m, (ACK-E10)	916606	Subtel	14.95 €
	Memory card	SDSDUNC-032G-GZFIN	SanDisk	9.99 €
	Mini HDMI to HDMI cable		AmazonBasics	6.00 €
Screen	TV 32″ Led HD	K32DLM7H	TD systems	139.00 €
TOTAL				18 670.49 €

[a] Note that the Bactronez anaerobic chamber includes: sleeves, elastic rubber sealing rings, sleeve compartment doors, integrated dry vacuum pump for the sleeve and the interlock purging, external lights, two sets of oxygen scrubber catalysts.

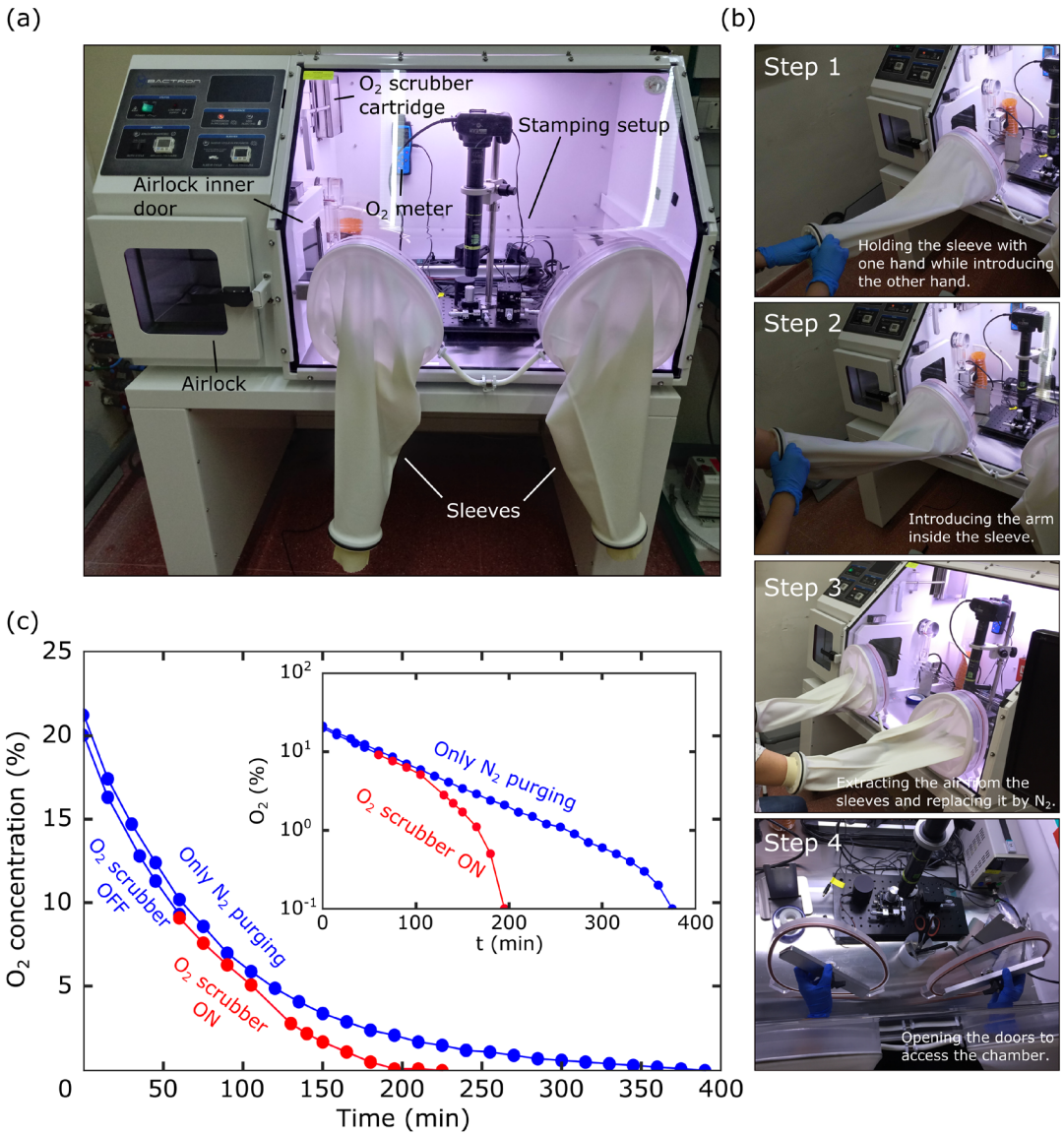

Figure 1. (a) Optical image of the gloveless chamber with the stamping setup mounted inside. (b) Optical images of the steps needed to introduce the hands inside the chamber. (c) Oxygen concentration drop in time within the chamber for a simple N_2 purging (blue dots line), and forming gas purging with the O_2 scrubber turned on after 50 min. (blue and red dots line). Inset: Oxygen concentration shown in log scale.

increasing substantially their cost and complexity of implementation [18].

Here, we present an alternative concept of deterministic transfer setup operated in inert conditions that is based on a gloveless anaerobic chamber. The user can operate inside the chamber using his/her bare hands without the need of thick glove-box gloves, making the transfer process virtually as easy as that carried out in air (outside the anaerobic chamber). Importantly, in the manuscript we provide all the details needed to facilitate the implementation of this system by other research groups.

Table 1 summarizes the different components needed to assemble our experimental system; whose cost is under the 20 000 €. We address the reader to the supp. info. (stacks.iop.org/TDM/7/025034/mmedia) for pictures of the different steps during the setup assembly process and for more details about the setup construction.

We build our transfer system within a gloveless anaerobic chamber (Bactronez 12.5). In order to access the interior part of the chamber, the system has two sealed doors connected to two plastic sleeves equipped with an elastic rubber sealing ring at their free end. The operator inserts his/her bare arms in the sleeves until feeling tight the rubber sealing ring around the arms like shown in figure 1(b). Then, the sleeves are pumped down and purged with N_2 three times. After this process, the operator can open the two sealed doors without altering the environmental conditions inside the chamber. The system is equipped with a scrubber cartridge with Pd coated pellets (which act as a catalyst) that actively remove O_2 from the chamber through the reaction $2H_2 + O_2 \xrightarrow{Pd} 2H_2O$ [19] when the system is purged with forming gas (N_2 + 5% H_2) mixture. The H_2O generated during the O_2 capture reaction is condensed in a big silica gel reservoir. We show in fig-

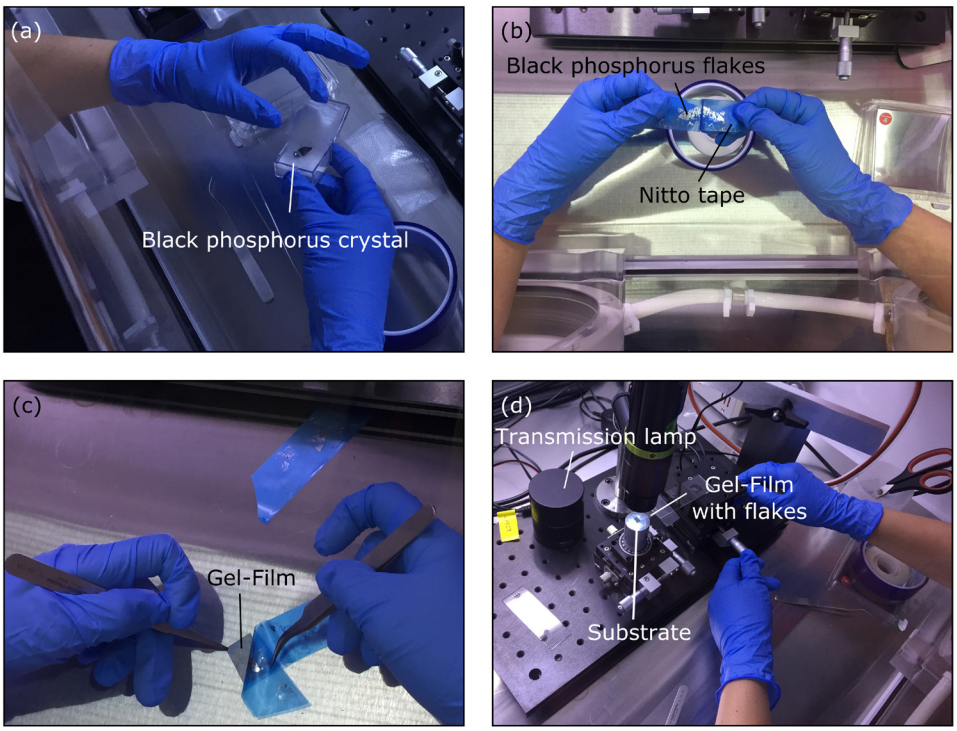

Figure 2. (a) Manipulation of the box with the bulk black phosphorus inside the chamber. (b) Mechanical exfoliation with Nitto tape by hand in the chamber. (c) Black phosphorus flakes being transferred onto the Gel-Film stamp after exfoliation with Nitto tape. (d) Handling the micrometer *XYZ* stage to deterministically transfer a flake.

ure 1(c) a comparison of the O_2 concentration evolution when the chamber is simply purged with N_2 (O_2 scrubber system OFF) and when the catalytic O_2 capture is employed (O_2 scrubber system ON). We found that the O_2 scrubber speeds up the O_2 concentration drop by a factor of 5 with respect to the simple N_2 purge. In fact, these kind of gloveless anaerobic chambers with active O_2 removal have proven to be very effective to generate environmental conditions with very low O_2 levels (in the 10 ppm range) [20].

Figure 2 shows how the operator is preparing a Gel-Film (WF ×4 6.0 mil, by Gel-Pak®) stamp with mechanically exfoliated black phosphorus. These pictures illustrate how the operator is able to easily carry out all the required delicate manual tasks (handling of tweezers, cutting, peeling, etc) as he/she does not need to wear thick glove-box gloves. Briefly, a bulk piece of black phosphorus (HQ Graphene) is exfoliated using Nitto SPV224 tape. The tape containing the exfoliated black phosphorus flakes is gently pressed against the surface of a rectangle piece of Gel-Film substrate that will be used as viscoelastic stamp for the deterministic transfer [2]. The stamp is secured overhanging in the edge of a microscope glass slide with Scotch tape (Magic tape) and the glass slide is fixed to a *XYZ* micro-manipulator stage, that will be used to move the stamp, with double side tape (Scotch restickable tabs). In order to identify the flake to be transferred, we place a collimated light source (Thorlabs quartz tungsten-halogen lamp, QTH11) under the stamp allowing us to infer the thickness of the flakes from its transmittance [21]. Once the desired flake is located, the lamp is replaced by an *XY*-rotation stage that will be used to move the acceptor sample (also fixed to the stage with double side Scotch restickable tabs).

Figure 3 shows a sequence of optical microscopy images acquired with the transfer system zoom lens during the deterministic placement of a black phosphorus flake onto a SiO_2/Si substrate with a pre-patterned alignment crosshair. First, the flake is aligned in the center of the crosshair markers. Then, the Gel-Film stamp is lowered until establishing a gentle contact between stamp and acceptor sample. Finally, the stamp is slowly peeled off until it is completely removed, and the flake is successfully transferred in the middle of the crosshair. The possibility to place flakes at a desired location (as shown in figure 3) can be further exploited to fabricate van der Waals heterostructures by stacking different 2D materials on top of each other. Figure 4 demonstrates the capability of our inert atmosphere deterministic placement system to fabricate this kind of artificial stacks of 2D materials. The different transfer steps to fabricate a heterostructure based on a few-layer black phosphorus (BP) flake sandwiched between two flakes of hexagonal boron nitride (hBN) are shown in figure 4.

In order to benchmark the potential of the gloveless anaerobic chamber to manipulate air-sensitive 2D materials, we monitor the evolution of the black phosphorus flake (transferred in figure 3) inside the anaerobic chamber through optical microscopy images with the system's zoom lens. Black phosphorus is well-

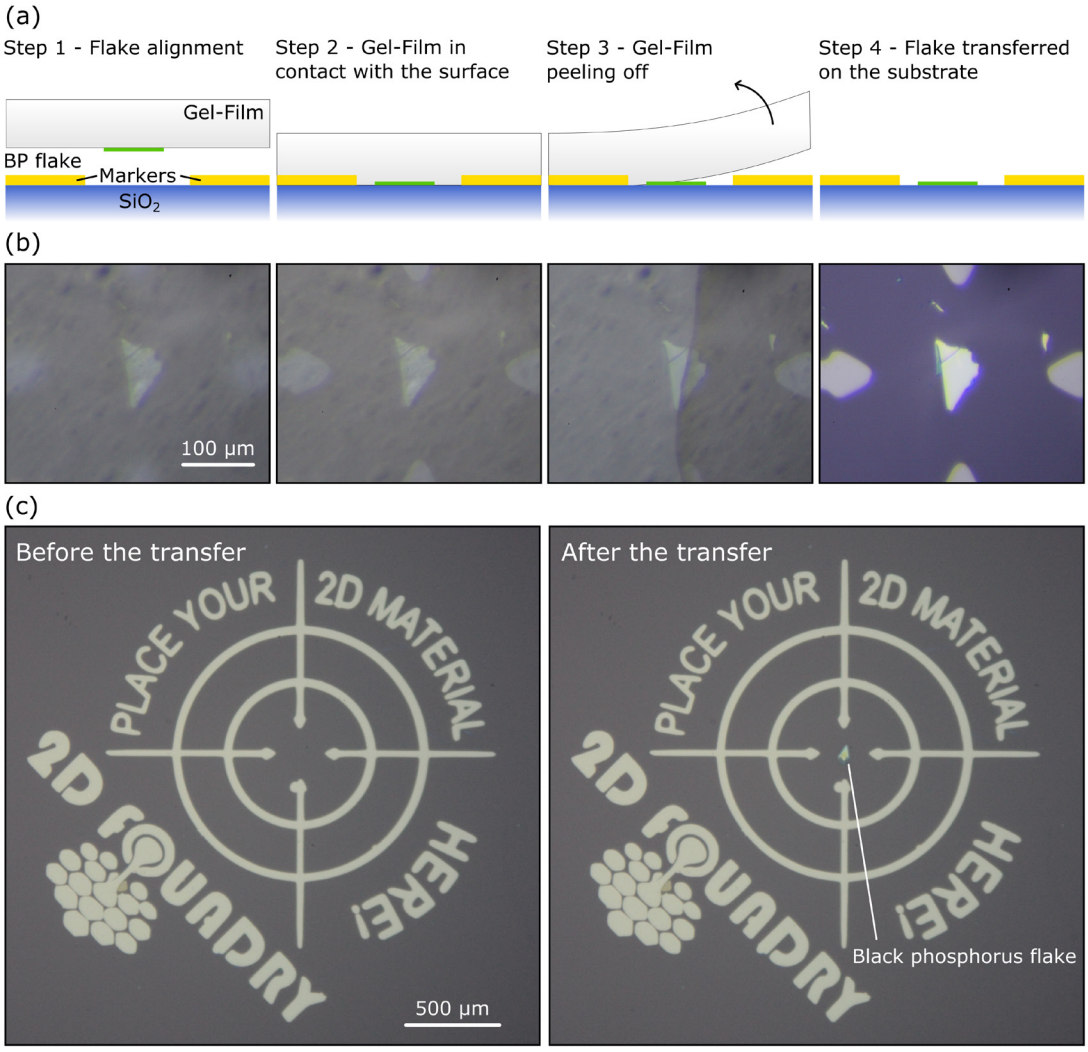

Figure 3. (a) Scheme of deterministic transfer process of black phosphorus flakes on marked substrates. (b) Optical images of the transfer of a black phosphorus flake in the gloveless chamber. (c) Optical images of the substrate before and after the transfer of the black phosphorus flake.

known for its instability under air exposure [22–24]. We do not notice any change in the optical microscopy images after 22 days inside the chamber. On the other hand, after taking the flake outside the chamber, it quickly shows signs of degradation from day 3 of air exposure (see inset in figure 5 with increased contrast) and it becomes severely damaged after 9 days of exposure. In figure 5, we show the optical contrast profiles acquired from the optical images of the black phosphorus sample along the black line indicated in the first panel. The profiles present a clear increase in roughness under air exposure due to the degradation, comparing with the profiles of the images of the flake inside the chamber. This illustrates the potential of this experimental setup for handling air-sensitive 2D materials.

Furthermore, we also checked the performance of the gloveless anaerobic chamber with even more unstable 2D materials. We studied a compound that belongs to the metal halide perovskites family that is known to quickly degrade upon atmospheric exposure [25–27]. The metal halide perovskites are a prominent group of materials in the solar harvesting research [28–30], optoelectronics [31–33] and photovoltaics [34, 35] which degrade rapidly when exposed to air or light [25, 36, 37]. In our case, the compound used is phenethylammonium lead iodide (PEA_2PbI_4) 2D perovskites synthesized according to the techniques described in [27, 38, 39]. The bulk crystals are exfoliated and transferred to a SiO_2/Si substrate inside the anaerobic chamber. Then, the sample is monitored for 5 h by acquiring microscope optical pictures, similar to the procedure used in the black phosphorus sample (figure 6). Again, no apparent change of the material is observed during the 5 h in inert atmosphere. However, the surface of the perovskite flakes quickly showed degradation signs after just 15 min outside the chamber. In this case, we show the optical contrast of the flake to illustrate the degradation upon air exposure (see the supporting information for the analysis of the time evolution of the optical contrast). Given the results, we conclude that the atmosphere in the anaerobic chamber allows the handling of very air-sensitive 2D materials.

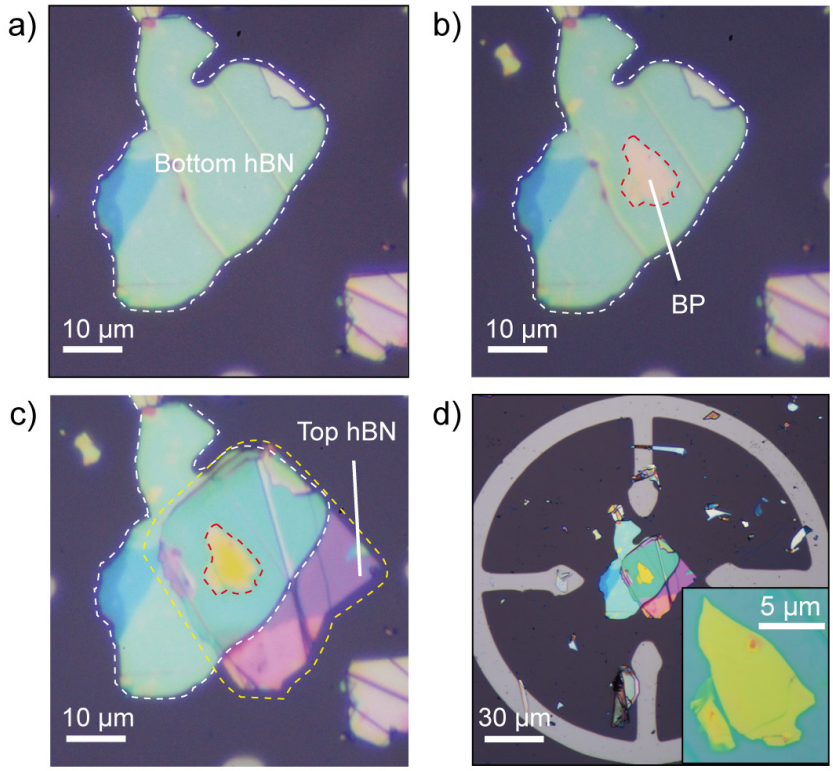

Figure 4. Fabrication of a van der Waals heterostructure under inert atmospheric conditions. (a) Optical image of hexagonal boron nitride (hBN) flake transferred onto a SiO_2/Si substrate. (b) black phosphorus (BP) flake transferred onto the boron nitride flake. (c) a top hBN flake is transferred to complete the hBN/BP/hBN stack. (d) A low magnification image of the assembled heterostructure in the middle of a crosshair marker. The inset shows a higher magnification optical microscopy image of the hBN/BP/hBN heterostructure.

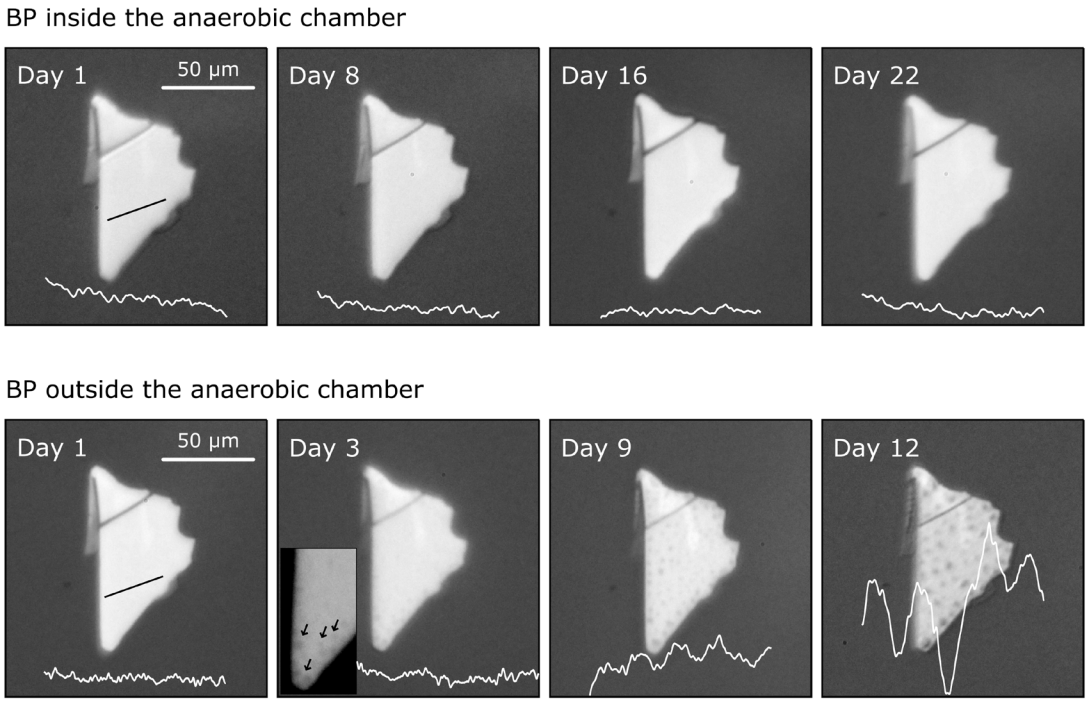

Figure 5. Optical images (showing the green channel which provides the highest contrast) of the same BP flake during several days inside the gloveless chamber (22 d) and outside it (12 d).

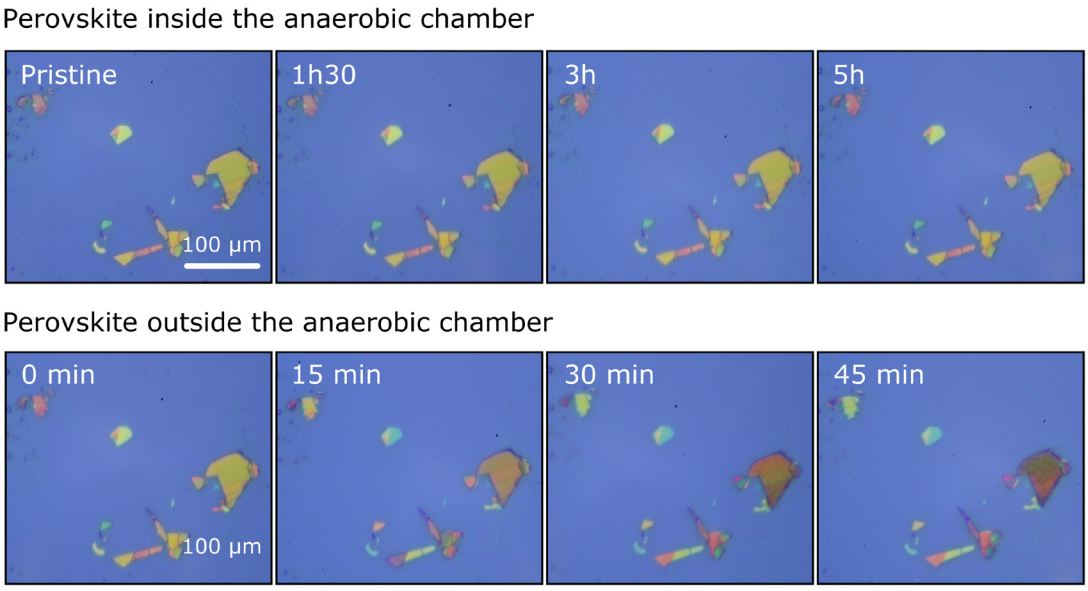

Figure 6. Optical images of the same perovskite flakes during several hours inside the gloveless chamber (5 h) and outside (45 min).

In summary, we have developed a system to precisely transfer 2D materials under inert atmosphere and we provide all necessary technical details to allow its implementation in other laboratories. Unlike other inert atmosphere transfer system used in the literature based on N_2 or Ar over pressurized gloveboxes, our system relies on a gloveless anaerobic chamber with an active O_2 catalytic capturing system. Our setup allows the operator to work with his/her bare hands within the chamber, which facilitate tasks as scissors cutting, tape peeling, tweezer handling, etc that are challenging to be done while wearing thick gloves required to access the interior of an over pressurized N_2 or Ar glove-box. We illustrate the operation of our transfer setup by showing the deterministic transfer of a black phosphorus flake and by studying the stability of thin black phosphorus and perovskite flakes. We believe that the simple operation and the low cost (<20 000 €) of this setup makes it highly attractive for other research groups that have not yet implemented a transfer system under inert atmosphere.

Acknowledgments

This project has received funding from the European Research Council (ERC) under the European Union's Horizon 2020 research and innovation programme (grant agreement n° 755655, ERC-StG 2017 project 2D-TOPSENSE). EU Graphene Flagship funding (Grant Graphene Core 2, 785219) is acknowledged. RF acknowledges the support from the Spanish Ministry of Economy, Industry and Competitiveness through a Juan de la Cierva-formación fellowship 2017 FJCI-2017-32919. QHZ acknowledges the grant from China Scholarship Council (CSC) under No. 201700290035. MS acknowledges the financial support of a fellowship from 'la Caixa' Foundation (ID 100010434). The fellowship code is LCF/BQ/IN17/11620040. MS has received funding from the European Union's Horizon 2020 research and innovation program under the Marie Skłodowska-Curie grant agreement No. 713673. FP acknowledges financial support from the Spanish Ministry of Economy and Competitiveness through the 'María de Maeztu' Program for Units of Excellence in R and D (MDM-2014-0377).

ORCID iDs

Patricia Gant https://orcid.org/0000-0002-0761-1627
Michael Seitz https://orcid.org/0000-0002-3515-1648
Ferry Prins https://orcid.org/0000-0001-7605-1566
Riccardo Frisenda https://orcid.org/0000-0003-1728-7354
Andres Castellanos-Gomez https://orcid.org/0000-0002-3384-3405

References

[1] Frisenda R *et al* 2018 Recent progress in the assembly of nanodevices and van der Waals heterostructures by deterministic placement of 2D materials *Chem. Soc. Rev.* **47** 53–68
[2] Castellanos-Gomez A *et al* 2014 Deterministic transfer of two-dimensional materials by all-dry viscoelastic stamping *2D Mater.* **1** 011002
[3] Li H, Wu J, Huang X, Yin Z, Liu J and Zhang H 2014 A universal, rapid method for clean transfer of nanostructures onto various substrates *ACS Nano* **8** 6563–70
[4] Dean C R *et al* 2010 Boron nitride substrates for high-quality graphene electronics *Nat. Nanotechnol.* **5** 722–6
[5] Schneider G F, Calado V E, Zandbergen H, Vandersypen L M K and Dekker C 2010 Wedging transfer of nanostructures *Nano Lett.* **10** 1912–6
[6] Zomer P J, Dash S P, Tombros N and Van Wees B J 2011 A transfer technique for high mobility graphene devices on

commercially available hexagonal boron nitride *Appl. Phys. Lett.* **99** 232104
[7] Wang L *et al* 2013 One-dimensional electrical contact to a two-dimensional material *Science* **342** 614–7
[8] Geim A K and Grigorieva I V 2013 Van der Waals heterostructures *Nature* **499** 419–25
[9] Liu Y, Weiss N O, Duan X, Cheng H-C, Huang Y and Duan X 2016 Van der Waals heterostructures and devices *Nat. Rev. Mater.* **1** 16042
[10] Frisenda R and Castellanos-Gomez A 2018 Robotic assembly of artificial nanomaterials *Nat. Nanotechnol.* **13** 441–2
[11] Haigh S J *et al* 2012 Cross-sectional imaging of individual layers and buried interfaces of graphene-based heterostructures and superlattices *Nat. Mater.* **11** 764–7
[12] Rooney A P *et al* 2017 Observing Imperfection in Atomic Interfaces for van der Waals Heterostructures *Nano Lett.* **17** 5222–8
[13] Kretinin A V *et al* 2014 Electronic properties of graphene encapsulated with different two-dimensional atomic crystals *Nano Lett.* **14** 3270–6
[14] Cao Y *et al* 2015 Quality heterostructures from two-dimensional crystals unstable in air by their assembly in inert atmosphere *Nano Lett.* **15** 4914–21
[15] Bandurin D A *et al* 2016 High electron mobility, quantum Hall effect and anomalous optical response in atomically thin InSe *Nat. Nanotechnol.* **12** 223–7
[16] Wang Z, Lin Q, Chmiel F P, Sakai N, Herz L M and Snaith H J 2017 Efficient ambient-air-stable solar cells with 2D–3D heterostructured butylammonium-caesium-formamidinium lead halide perovskites *Nat. Energy* **2** 17135
[17] Tan S J R *et al* 2018 Quasi-monolayer black phosphorus with high mobility and air stability *Adv. Mater.* **30** 1704619
[18] Masubuchi S *et al* 2018 Autonomous robotic searching and assembly of two-dimensional crystals to build van der Waals superlattices *Nat. Commun.* **9** 1413
[19] Nyberg C and Tengstål C G 1984 Adsorption and reaction of water, oxygen, and hydrogen on Pd(1 0 0): identification of adsorbed hydroxyl and implications for the catalytic H_2–O_2 reaction *J. Chem. Phys.* **80** 3463–8
[20] Sudo S Z and Hersch P A 1974 Monitoring the atmosphere in an anaerobic chamber *Appl. Environ. Microbiol.* **28** 582–5
[21] Taghavi N S *et al* 2019 Thickness determination of MoS_2, $MoSe_2$, WS_2 and WSe_2 on transparent stamps used for deterministic transfer of 2D materials *Nano Res.* **12** 1691–5
[22] Castellanos-Gomez A 2015 Black phosphorus: narrow gap, wide applications *J. Phys. Chem. Lett.* **6** 4280–91
[23] Island J O, Steele G A, Van Der Zant H S J and Castellanos-Gomez A 2015 Environmental instability of few-layer black phosphorus *2D Mater.* **2** 011002
[24] Gamage S *et al* 2016 Nanoscopy of black phosphorus degradation *Adv. Mater. Interfaces* **3** 1600121
[25] Berhe T A *et al* 2016 Organometal halide perovskite solar cells: Degradation and stability *Energy Environ. Sci.* **9** 323–56
[26] Fang H *et al* 2018 Unravelling light-induced degradation of layered perovskite crystals and design of efficient encapsulation for improved photostability *Adv. Funct. Mater.* **28** 1800305
[27] Seitz M, Gant P, Castellanos-Gomez A and Prins F 2019 Long-term stabilization of two-dimensional perovskites by encapsulation with hexagonal boron nitride *Nanomaterials* **9** 1120
[28] Antonietta Loi M and Hummelen J C 2013 Hybrid solar cells: perovskites under the Sun *Nat. Mater.* **12** 1087–9
[29] Stranks S D and Snaith H J 2015 Metal-halide perovskites for photovoltaic and light-emitting devices *Nat. Nanotechnol.* **10** 391–402
[30] Zhang W, Eperon G E and Snaith H J 2016 Metal halide perovskites for energy applications *Nat. Energy* **1** 16048
[31] Manser J S, Christians J A and Kamat P V 2016 Intriguing optoelectronic properties of metal halide perovskites *Chem. Rev.* **116** 12956–008
[32] Zhao Y and Zhu K 2016 Organic-inorganic hybrid lead halide perovskites for optoelectronic and electronic applications *Chem. Soc. Rev.* **45** 655–89
[33] Chen Q *et al* 2015 Under the spotlight: the organic–inorganic hybrid halide perovskite for optoelectronic applications *Nano Today* **10** 355–96
[34] Kojima A, Teshima K, Shirai Y and Miyasaka T 2009 Organometal halide perovskites as visible-light sensitizers for photovoltaic cells *J. Am. Chem. Soc.* **131** 6050–1
[35] Gao P, Grätzel M and Kazeeruddin M 2014 Environmental Science Organohalide lead perovskites for photovoltaic *Energy Environ. Sci.* **1** 2448–63
[36] Domanski K *et al* 2016 Not all that glitters is gold: metal-migration-induced degradation in perovskite solar cells *ACS Nano* **10** 6306–14
[37] Ahn N *et al* 2016 Trapped charge-driven degradation of perovskite solar cells *Nat. Commun.* **7** 13422
[38] Yaffe O *et al* 2015 Excitons in ultrathin organic-inorganic perovskite crystals *Phys. Rev.* B **92** 045414
[39] Ha S T, Shen C, Zhang J and Xiong Q 2016 Laser cooling of organic–inorganic lead halide perovskites *Nat. Photon.* **10** 115–21